Hindawi
Geofluids
Volume 2022, Article ID 3226001, 14 pages
https://doi.org/10.1155/2022/3226001

Research Article

Thermal Environment and Energy Performance of a Typical Classroom Building in a Hot-Humid Region: A Case Study in Guangzhou, China

Liang Yi,[1] Yuan Xie,[1] and Chang Lin[2]

[1]School of Architecture, South China University of Technology, Guangzhou 510641, China
[2]Guangzhou Academy of Fine Arts, Guangzhou 511400, China

Correspondence should be addressed to Chang Lin; linchang@gzarts.edu.cn

Received 19 May 2022; Revised 1 July 2022; Accepted 11 July 2022; Published 30 July 2022

Academic Editor: Guang-Liang Feng

Buildings and the construction sector account substantially for global energy consumption. In hot-humid areas of China, suboptimal thermal comfort in classrooms has heightened their cooling load and energy consumption. It is necessary to renovate the buildings of outdated code according to the current weather conditions to save energy. This study thus aimed to examine the thermal effects of such designs on the cooling load, based on an actual classroom building during summers in hot-humid southern China. Using air temperature and PMV values to evaluate thermal comfort, this study conducted simulation through EnergyPlus and DesignBuilder. The resultant updated typical meteorological year (TMY) and the monthly and hourly analyses of indoor thermal comfort revealed persistent classroom overheating. To mitigate the cooling load, numerous design variables were investigated: space form, roofing, external walls, windows, and shading devices. Evaluative comparisons found that appropriate choice of external windows and shading devices represented the two most effective strategies in mitigating the cooling load. Furthermore, jointly applying effective retrofit strategies to the building yielded a favorable reduction in the annual cooling energy consumption by 16.6%. The findings herein are envisioned to provide evidence-based referential guidance for building designs for classrooms in a hot-humid climate.

1. Introduction

Across the globe, buildings and the construction sector collectively constitute a substantial share of the total energy consumption. In 2010, more than one third of the total global final energy was accounted for by buildings, highlighting their role as the dominant end-use sector worldwide [1]. More specifically, building energy consumption represented 20–40% [2] of the total energy use for developed countries and 20.7% [3] in 2004 for China. The energy demand by buildings has been projected to continue its upward trajectory in future [4–8]. Additionally, it is noteworthy that energy-related CO_2 emissions from buildings have escalated in recent years. In 2019, unprecedentedly high levels were reported for direct and indirect emissions from electricity and commercial heat used in buildings [9]. Accordingly, improving the energy efficiency of buildings has been regarded as a strategy to reduce both energy consumption and CO_2 emissions.

Educational buildings such as classrooms, an integral part of campus life [10], have been shown to affect students' health and performances through thermal comfort [11–13]. This is exemplified by Guangzhou, a city in southern China, characterized by long, hot-humid summers and short-warm winters. In such a climate, the indoor environment of naturally ventilated buildings is usually unsatisfactory because of high temperature, high humidity, and strong radiation.

Under the restriction of economic and technical conditions, the air conditioning system was not popularized in the local area before the twenty-first century. Under natural ventilation, good building heat dissipation capacity is very important for prolonging indoor comfort time. With the rising temperature and economic development, most local buildings are now equipped with air conditioning systems to cope with the hot climate. However, as far as the current climate is concerned, most of the old buildings are not properly insulated, resulting in an unnecessary large amount of cooling load. In order to reduce energy and carbon emissions, it is necessary to transform old buildings to improve energy efficiency. We take a typical teaching building constructed in the early stage as a case study. To ensure indoor comfort during summers, heating, ventilation, and air conditioning (HVAC) systems are needed. Because of the hot and humid climate, generally, buildings in hot and humid areas in China do not have heating equipment. Building energy in this area is dominated by cooling load [14–18]. The widespread use of such HVAC systems, coupled with the rapid growth in the numbers of campuses and students in China (Figures 1 and 2) [19], suggests that the energy consumption will continue to escalate [20]. Hence, exploring methods to reduce the cooling load and, in turn, energy consumption of classrooms in hot-humid areas has become a challenge faced by not only governments and educational institutions, but also architects [21].

Architecture critically governs energy performances of buildings and thermal comfort of their inhabitants [22–24]. Optimizing the thermal performance of the envelope [25, 26] and increasing the sunshade construction can save the cooling load [27, 28]. In the context of campus life, the prudent use of passive design and HVAC systems enables energy savings in certain climates [29] and offers a thermally comfortable and conducive environment for students' activities. To this end, energy simulation tools such as EnergyPlus [5] have commonly been used: Through meteorological data and modeling of buildings, such tools can yield intuitive calculations on building performances. Such simulation results may then be compared to examine the influences of design variables on the performances.

Against this background, the objective of this study was to investigate the thermal environment and the cooling load of classroom buildings during summers in hot-humid areas of southern China. The aims were as follows: (1) to examine the thermal comfort of naturally ventilated classrooms under typical summer weather conditions; (2) to analyze the cooling load of the classrooms throughout the year; (3) to estimate the saving potential for the cooling load of classrooms by testing the impacts of different design variables; and (4) to provide evidence-based referential guidance for building designs for classrooms in a hot-humid climate.

2. Materials and Methods

2.1. Study Area. The study area is a seven-story classroom building in the South China University of Technology, Guangzhou (Figure 3). This building is made of bricks and concrete blocks. One side of the corridor is a classroom, and the other side is open to the outdoor environment. This semi-open corridor space is common in buildings built at the end of last century, because it can provide shade and air convection without affecting the building space (Figure 4). The classrooms were on the north and south sides and occupied the second story and above, at a height of 3.6 meters. In the east-west direction, the distance between pillars was 4 meters. The windows, each 2.0 meters high, were positioned between the pillars on the facade of the building, while the roofs were furnished with green roofs for thermal insulation. Simulation-based investigations were undertaken for the thermal environment of the classrooms under natural ventilation and for the cooling load of those under air conditioning.

2.2. Thermal Comfort Evaluation Criteria. Two types of evaluative indicators for indoor thermal comfort have globally been used: simple physical indices and complex computational indices. The physical indices are intuitive and easy for users, as exemplified by the air temperature. Evidence has suggested that the 80% acceptable upper limit of indoor temperatures is 29.5°C [30, 31] for naturally ventilated buildings in hot-humid areas of China. Accordingly, the temperature of 29.5°C was designated in this study as one of the upper limits of thermal comfort; any classroom temperatures above it would be considered overheating.

The other indicator is the relatively complex indices generated by calculations of environmental and human response variables. Examples include the predicted mean vote (PMV) index and physiological equivalent temperature (PET) index. For the PMV model [32] established by Fanger, its fundamental basis encompasses human thermal balance and subjective thermal sensation in psychophysiology. As a composite index of thermal comfort, the PMV index considers factors such as the relative humidity, mean radiant temperature (MRT), wind speed, metabolic rate, and clothing insulation. To denote human sensation, a range from -3 (extreme cold) to 3 (extreme hot) is used. Across this range, values between -0.5 and 0.5 correspond to 90% acceptability of thermal comfort, while those between -0.85 and 0.85 [33, 34] correspond to 80%. Accordingly, a PMV value of 0.85 was designated in this study as another upper limit of thermal comfort. One further practical consideration concerns the criticism for the PMV model on its inaccuracies when applied to naturally ventilated buildings in warm areas [33, 35, 36]. To address this for enhanced applicability of the model, an expectancy factor has thus been recommended in the literature for calculations [37]: This enables its adaptive modification to more accurately characterize local areas based on field research. Thus, in this study, an expectancy factor of 0.822 (based on local research) was included in calculating thermal comfort [38].

2.3. Simulations

2.3.1. Dynamic Building Simulation Engine. To investigate the thermal environment and long-term cooling load of classrooms in hot-humid areas, a numerical simulation tool known as EnergyPlus was used in this study. Developed by the US Department of Energy's Building Technologies Office, EnergyPlus [39] is a whole-building energy simulation program, whose accuracy has been validated by many studies [40–46]. Over the years, it has been widely used in building simulations worldwide, including hot-humid areas [47–50]. For convenient and practical use of EnergyPlus, user interfaces are usually coupled to it: This study accordingly used DesignBuilder

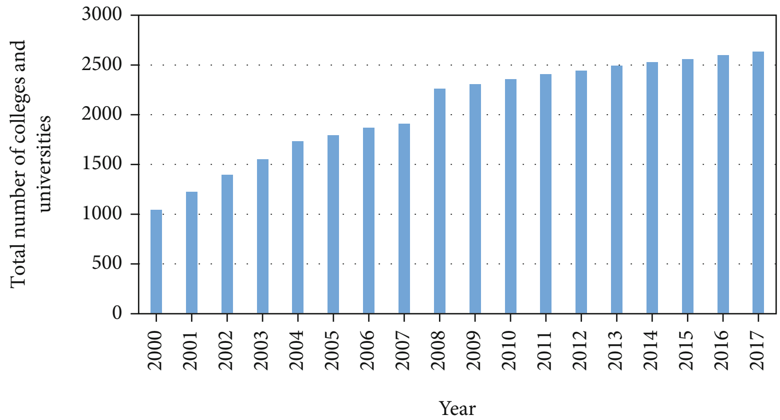

Figure 1: Increase of Chinese colleges and universities.

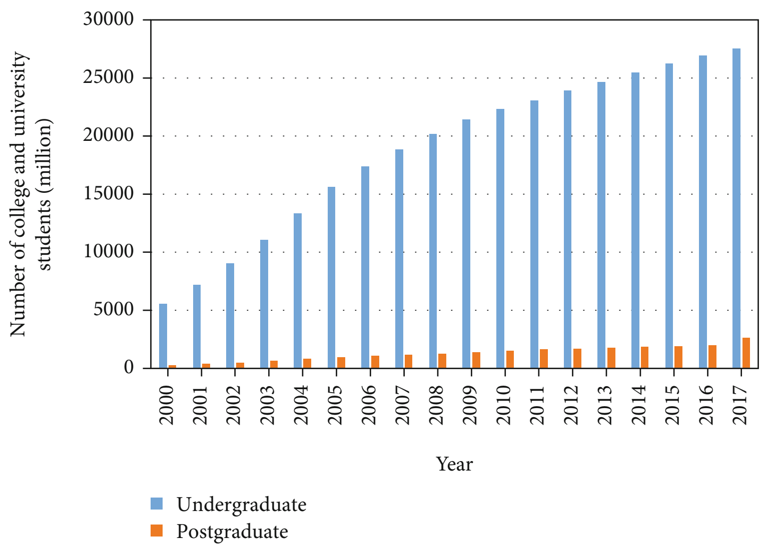

Figure 2: Increase of colleges and universities students.

Figure 3: The seven-story classroom building under investigation.

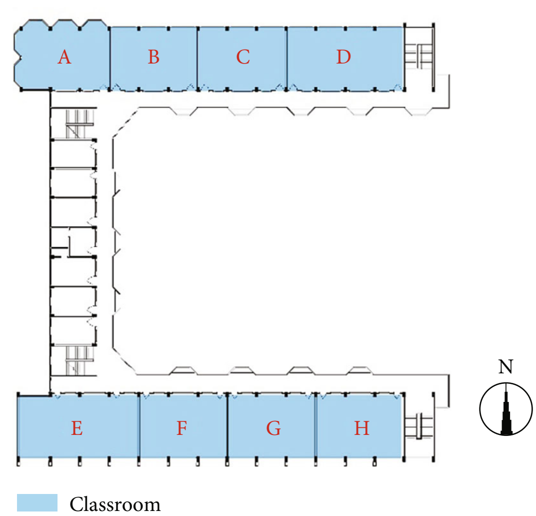

Figure 4: The building plan of the classrooms.

[51] (software version V6), an established and advanced user interface, for the simulation.

2.3.2. Weather Data. To reliably simulate energy consumption, hourly meteorological data are necessary [52]. A useful conceptualization in this context is the typical meteorological year (TMY): It represents the one-year collation of hourly meteorological and solar data for a location based on longer periods of time, accurately reflecting its local climate. In the hot-humid region, building energy consumption is dominated by cooling demand. Under the context of global warming and climate change, it would be more accurate for building energy evaluations to take the impacts of the two internal factors into consideration. This study, a TMY file spanning the period from 2007 to 2016 of Guangzhou, was established, incorporating ten-year hourly meteorological and solar data from the NOAA and PVGIS databases [53], respectively.

To generate the TMY, the Sandia method (developed by Sandia National Laboratories [54]) was adopted. It used the Finkelstein-Schafer (FS) statistical method to consider weather variables in the calculations. The FS value characterized the difference between a specific weather variable in a certain month and in a long-term period. By assigning proper weights to the weather variables, the weighted-sum value of every single candidate month could be calculated: A lower WS value indicated a smaller deviation between the monthly weather and the long-term climate. The FS and WS were calculated based on the following equations:

$$\mathrm{FS}_W = 1/\mathrm{n} \sum_{i=1}^{n} \delta_{i,W}, \quad \mathrm{WS} = \sum w_i \times \mathrm{FS}_W, \tag{1}$$

where $\delta_{i,w}$ is the absolute difference between the long-term cumulative distribution function (CDF) of the weather variable w and that of the candidate month, n is the number of days of the candidate month, and w_i is the weight of w. (As recommended by the National Renewable Energy Laboratory, the maximum and minimum dry bulb temperature, maximum and minimum humidity, and maximum and mean wind velocity account for 1/20 of the weight; the mean dry bulb temperature and mean humidity account for 2/20; and the global and direct radiations account for 5/20 [55].)

A simple persistence process was used to choose the best month to form the TMY among the five candidate months with lower WS statistics. The process, referred to as the Pissimanis method [56], calculated the root mean square difference (RMSD) of the global radiation of the candidate month. Accordingly, the month with the minimum RMSD was selected as the typical meteorological month (TMM). The algorithm was as follows:

$$\mathrm{RMSD} = \left[\sum_{i=1}^{n} \left(H_{y,m} - \bar{H}_m \right) / n \right]^{1/2}, \tag{2}$$

where n is the number of days of the candidate month; $H_{y,m,i}$ is the daily global radiation of a certain day; y, m, and i are the specific year, month, and day; and $\bar{H}_m$ is the long-term mean value for daily global radiation.

Since TMMs were selected from different years, curve fitting techniques were applied to the six hours at the beginning and end of each month, to ensure smooth data transition between the months. The average temperature and daily radiation of Guangzhou were thus obtained, which illustrate the general characteristics of hot summer and warm winter regions (Figures 5 and 6).

2.3.3. Model Settings. The model setting of the building is based on previous research and common engineering practices, to achieve the goal of being as close to reality as possible. Constructions layers (from external interface to internal) and the U value of the building parts are outlined in Table 1. Those construction layers with a thickness less than 3 mm were excluded from calculations. The green roof settings are outlined in Table 2. The building model is shown in Figure 7.

In this study, summer vacation began on 16 July and ended on 31 August. The classroom were in use daily from 8 : 00 to 21 : 00 (they were used for teaching during the day and served as study areas at night). Occupancy in classrooms was set to 0.6 people/m^2 for most of the time, but was reduced to 0.5 people/m^2 for two periods (12 : 00 to 14 : 00 and 17 : 00 to 18 : 00) to account for the breaktime. Other relevant parameters were as follows: metabolic rate for a seated human body in summer (1.1 met); clothing insulation for a seated human body in summer (0.5 clo); air change rate (5 times per hour); air infiltration constant rate (0.7 ac/h); light density power (9 W/m^2); and other equipment power density (5 W/m^2). According to local customs, air conditioning systems of the classrooms were switched on from May to October, during which the average daily outdoor temperature was above 25°C. The cooling set point was 26°C in the simulation models.

To analyze the impacts of architectural designs on the cooling load of classroom buildings in hot-humid areas, various aspects of renovation were investigated: the space form, roof construction, wall construction, window materials, and additional shading devices. Different models were made, for each of which one design variable was altered in comparison to the benchmark model. Following this, differences in the resultant cooling load were quantified to determine the extents of their impacts in the hot-humid climate. Furthermore, synergistic strategies were generated to further explore the cooling load saving potential of the buildings.

3. Results and Discussion

3.1. Thermal Comfort in Naturally Ventilated Classrooms

3.1.1. Relationship between Indoor Temperatures and Outdoor Temperatures. The relationships between daily indoor temperatures in naturally ventilated classrooms and outdoor temperatures were examined for summer days on which the classrooms were occupied (Figures 8–10). The scatter plots outline the indoor and outdoor temperatures during classes in a single day, with each data point representing each of the 98 days of summer class. One of our findings was that the indoor temperatures rose linearly with the outdoor ones. Another finding was that, throughout the summer, the average temperatures in the classroom were mostly above 29.5°C, clustering in the range from 30°C to 35°C. The highest

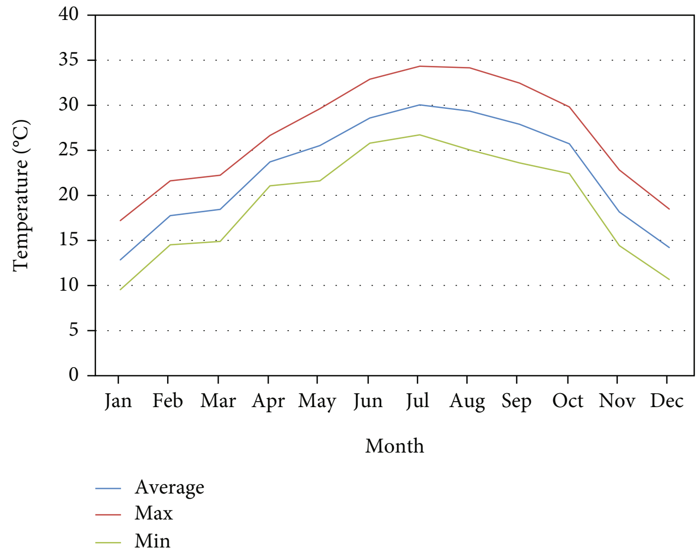

Figure 5: Average temperature.

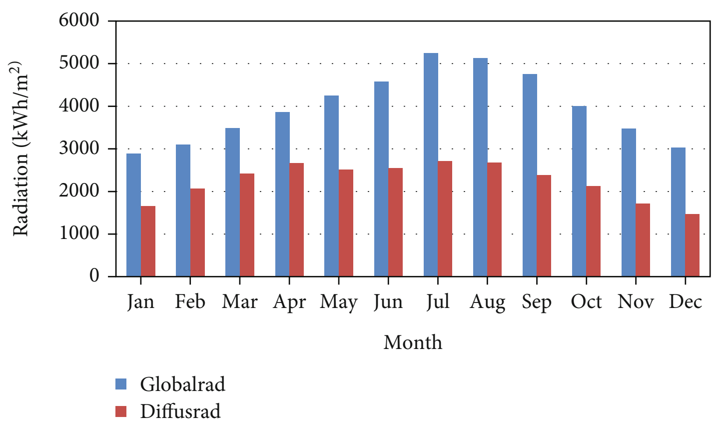

Figure 6: Daily average radiation.

temperature was close to 37.5°C, whereas the lowest was above 22.5°C. Furthermore, the indoor temperatures were generally higher than outdoor ones. Lastly, elevated indoor temperatures were observed for higher floors. Within the building, the seventh floor registered the highest temperatures, reflecting the least thermally comfortable environment under natural ventilation. Conversely, the second registered the lowest, reflecting its greatest thermal comfort.

3.1.2. Monthly Analysis of Indoor Thermal Comfort. Monthly analysis of indoor thermal comfort was undertaken based on the monthly average indoor temperatures and PMV values (Figures 11 and 12). The average indoor temperatures were above the threshold for thermal comfort across the five months of summer: Those of May and October were lower than June, July, and August. For the maximum indoor temperatures, the readings of all five months were above the threshold (with the highest exceeding 37°C being observed in June); for the minimum ones, they were all below the threshold. Likewise, the average PMV values were above the threshold for thermal comfort across all five months, with those of June, July, and September exceeding 2.0. For the maximum PMV values, the readings of all five months were above the threshold (with those from May to October being close to 3.0); for the minimum ones, the readings of only June and July were above it.

Further analysis focused on the percentage of time of thermal discomfort. The PMV-based evaluation criteria were more stringent than the temperature-based ones: The percentages calculated by the PMV method for all the months were higher than those calculated by temperatures (Figures 13 and 14). Comparison between the months found that, for May, the lowest percentage of uncomfortable time was observed. For June and July, the highest percentages were observed, for which the PMV values reached almost 100%. For September and October, though the percentages were lower, the values were nonetheless high, indicating almost constant overheating in the classrooms. Further

Table 1: Building parts.

Building parts	Construction layer	Thickness (m)	U value
External wall	Gravel	0.015	2.020
	Mortar	0.015	
	Brick	0.18	
	Gypsum plastering	0.01	
Internal wall	Gypsum plastering	0.01	1.821
	Brick	0.18	
	Gypsum plastering	0.01	
Roof	Soil	0.30	1.472
	Mortar	0.02	
	Concrete	0.05	
	Mortar	0.02	
	Mortar	0.02	
	Mortar	0.03	
	Concrete reinforced	0.10	
	Gypsum plastering	0.01	
Internal floor	Terrazzo	0.01	2.495
	Concrete reinforced	0.10	
	Gypsum plasterboard	0.02	
Glazing	Glass	0.03	5.894

Table 2: Green roof setting.

Height of plants(m)	0.30
Leaf area index	2.00
Leaf reflectivity	0.22
Leaf emissivity	0.95
Minimum stomatal resistance(s/m)	180.00
Max volumetric moisture content at saturation	0.50
Min residual volumetric moisture content	0.01
Initial volumetric moisture content	0.15

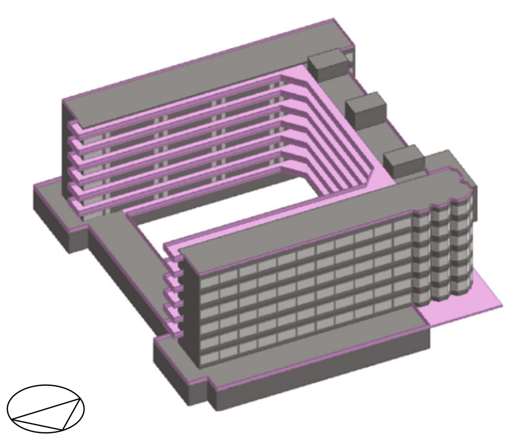

Figure 7: Building model.

comparison between the floors found that the proportion of uncomfortable time rose progressively with the height of the floor. Lastly, among all the floors, the classrooms on the second floor evidently registered the greatest thermal comfort.

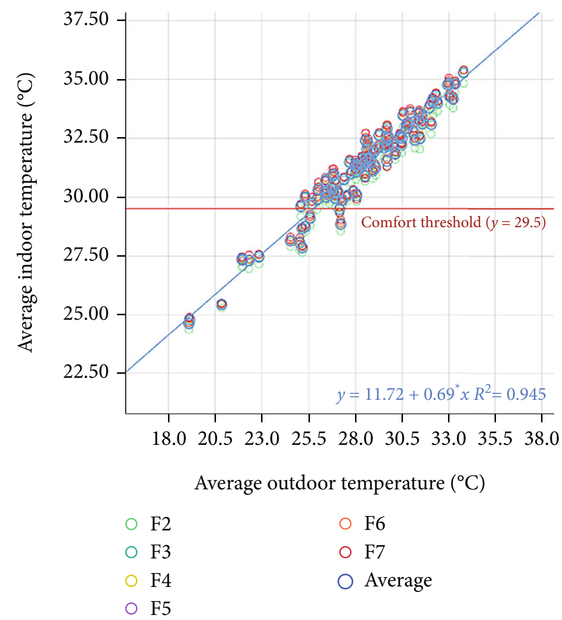

Figure 8: Daily average indoor temperatures in relation to average outdoor temperatures.

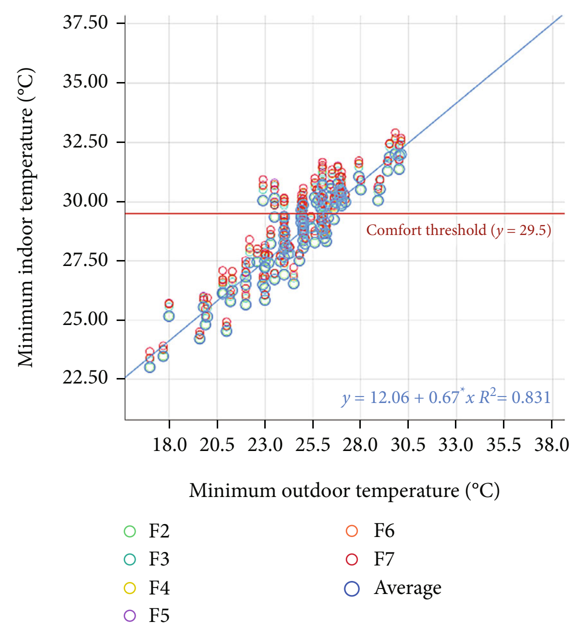

Figure 9: Daily minimum indoor temperatures in relation to minimum outdoor temperatures.

3.1.3. Hourly Analysis of Indoor Thermal Comfort. Hourly analysis of indoor thermal comfort determined that the box plots for indoor temperatures and PMV values exhibited similar trends during a summer day (Figures 15 and 16). Based on both temperatures and PMV values, the most comfortable time of the day in the classroom was 9 : 00; this was followed by a rise to the peak at 17 : 00 and then a gradual decline until 21 : 00. With temperatures as the evaluative criterion, only the median line of the 9 : 00 hourly interval and the lower quartiles of both 10 : 00 and 11 : 00 hourly intervals

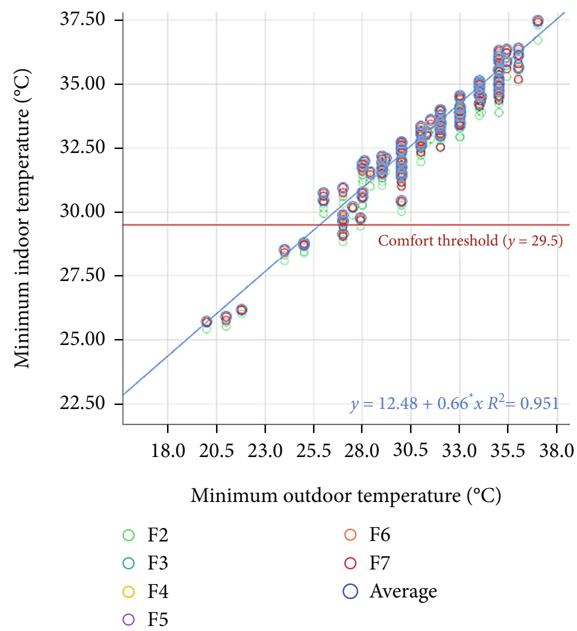

Figure 10: Daily maximum indoor temperatures in relation to maximum outdoor temperatures.

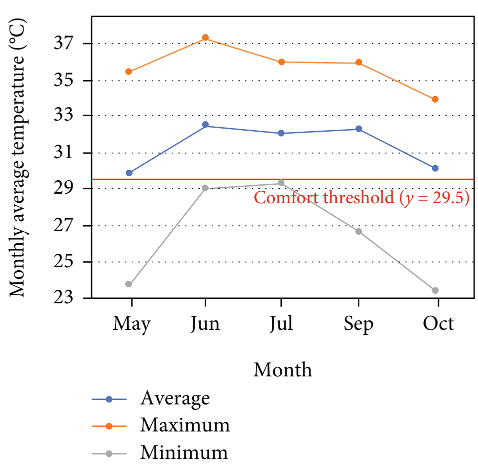

Figure 11: Monthly average temperature.

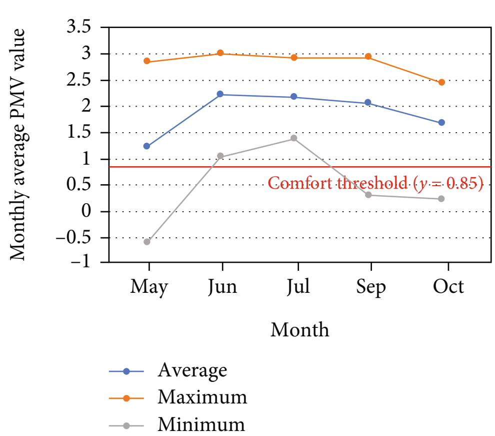

Figure 12: Monthly average PMV.

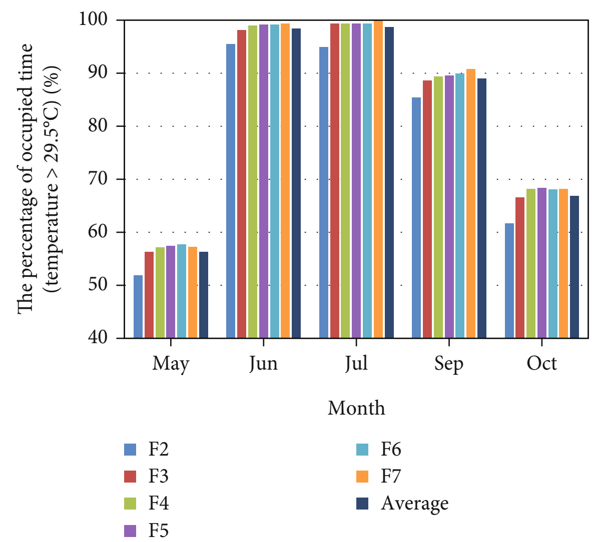

Figure 13: The percentage of time of thermal discomfort (based on temperature >29.5°C).

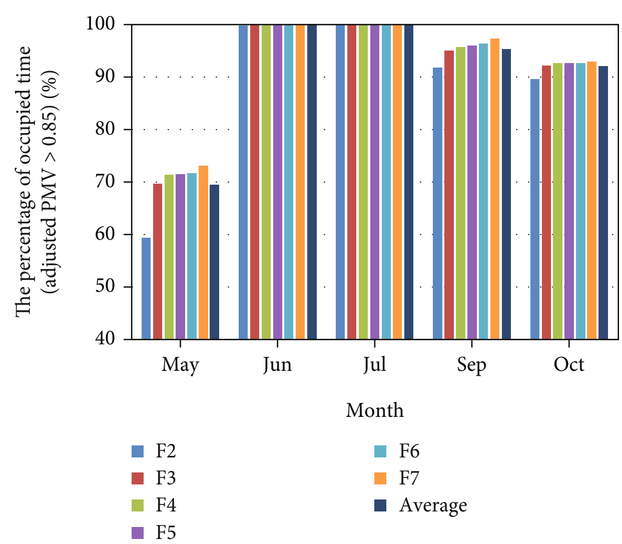

Figure 14: The percentage of time of thermal discomfort (based on PMV >0.85).

were lower than the threshold of 29.5°C. The reverse was true for all other data points. With PMV values as the criterion, only the lower quartiles of nine of the hourly intervals barely met the requirement of thermal comfort.

3.2. Cooling Load of Air-Conditioned Classrooms. The annual cooling load for the 48 classrooms was 888.3 MWh. Given the operation time (93 days × 13 hours per day), and the cooling energy consumption per square meter per hour was 128.3 W. The cooling load of the classrooms increased from the lowermost floor to the uppermost: The topmost classrooms incurred a cooling load of 155.3MWh, while bottommost classrooms incurred 136.7 MWh, which was only 88% of the topmost ones.

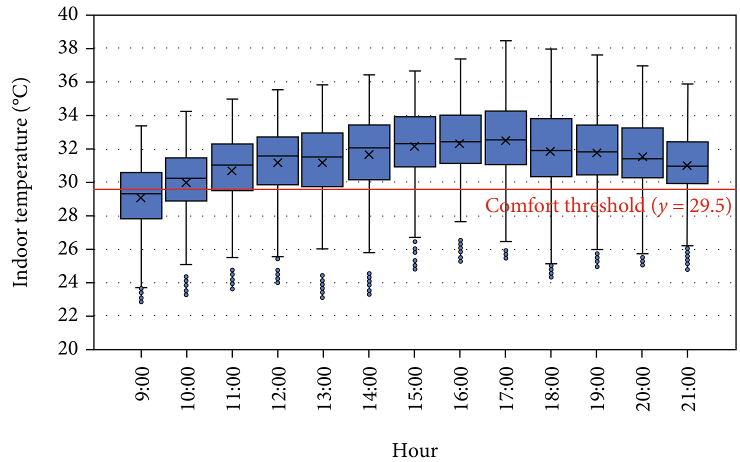

FIGURE 15: Indoor temperatures at hourly intervals.

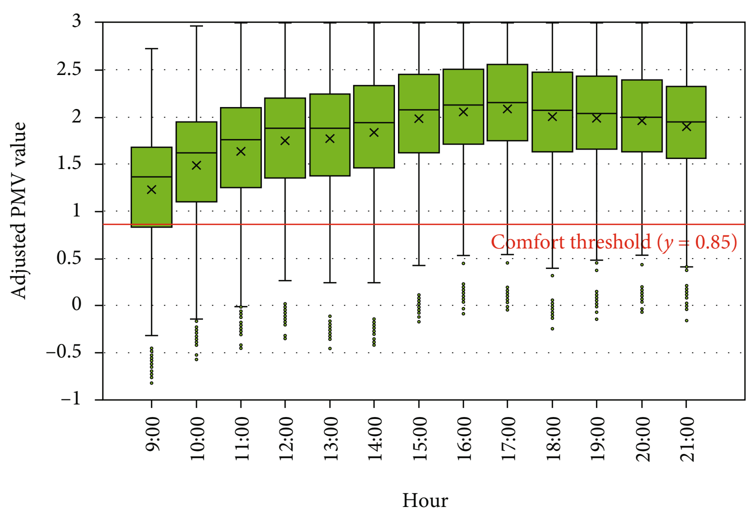

FIGURE 16: Indoor PMV values at hourly intervals.

3.2.1. Space Form. The designs of facades and the presence of windows are known to affect the cooling load of buildings. For each floor of the building, classroom A (Figure 4) on the northwest corner had concave-convex facades and windows on the west facade. To understand the thermal significance of the facades and windows, comparisons were drawn based on several retrofit plans. In case 1, the windows on the west facade were eliminated for reduced direst entry of solar radiation in the afternoon. In case 2, the concave-convex facades were replaced with regular flat ones. Case 3 represented a combination of cases 1 and 2 (Figure 17). It is noteworthy that, because the irregular layout had not been easy to use in the first place, the reduced indoor area arising from changes in cases 1 to 3 exerted negligible effect on the use of the classrooms.

The resultant changes of the total cooling load of the five classrooms and of the entire building were computed. The findings showed that the retrofit measures effectively reduced the annual cooling energy consumption of these classrooms. Compared with the original case, the cooling load of the classrooms in the three cases has, respectively, declined by 6.6%, 8.8%, and 15.4%. Moreover, the cooling loads of the entire building in the three cases were 99.0%, 98.8%, and 97.8% of the original.

3.2.2. Roof Construction. Given the role of solar radiation as the predominant heat source for the topmost floors [57], roof construction crucially governed the thermal comfort and HVAC energy consumption of indoor spaces at those floors [58, 59]. In this context, green roofs have been reported in the literature to contribute to diminished cooling load in hot-humid areas [60–62]. Passive designs as green roofs and thermal conductivity are common in the locality. To understand the thermal significance of roofing, comparisons were drawn with respect to the original case involving green roofs without thermal insulation. By changing the thickness of such insulation, the thermal transmittance (denoted by the U value) of the roofs was analyzed (Table 3).

The results showed that both the installation of green roofs and thermal insulation lessened the cooling load. Case 4 illustrated that, in the absence of green roofs and thermal

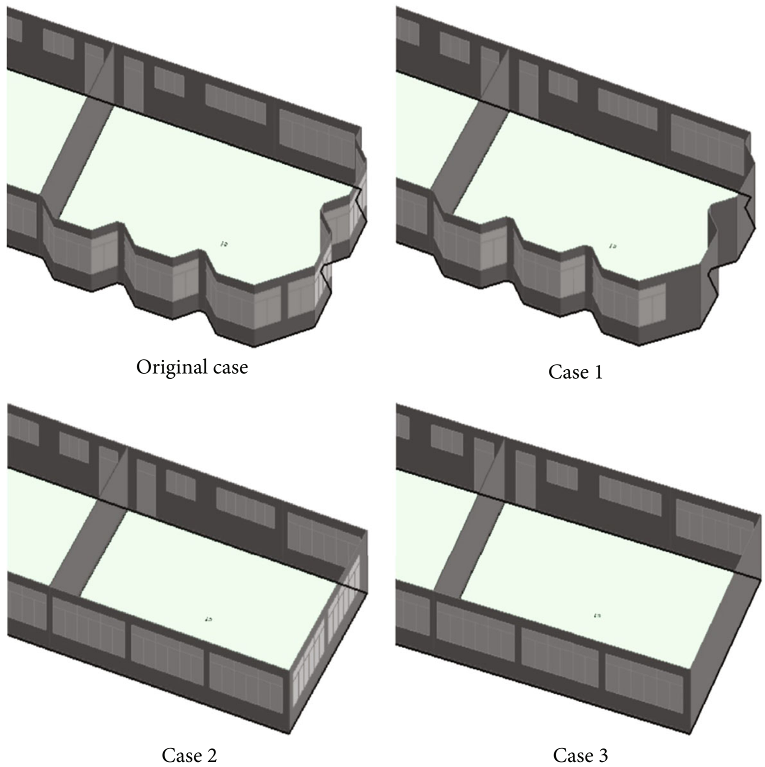

Figure 17: Space form of classroom A.

Table 3: Roof construction of cases 4 to 14.

Case	Thickness of thermal insulation (m)	Green roof	U value
Original case	0	Yes	0.725
Case 4	0.05	No	0.547
Case 5	0.075	No	0.39
Case 6	0.1	No	0.303
Case 7	0.05	Yes	0.353
Case 8	0.075	Yes	0.28

Table 4: External wall construction of cases 15 to 25.

Case	Envelope material	Thickness of thermal insulation (m)	U value
Original case	Ordinary brick	0	2.02
Case 10	Aerated brick	0	0.605
Case 11	Aerated brick	0.02	0.464
Case 12	Aerated brick	0.04	0.377
Case 13	Aerated brick	0.06	0.317
Case 14	Aerated brick	0.08	0.274
Case 15	Aerated brick	0.1	0.241

insulation, the cooling load of the topmost classrooms increased by 2.5%. Nonetheless, the most energy-efficient roof construction was not the one with both green roofs and thermal insulation. Of all the cases, case 7 with the thermal insulation of 0.1 m registered the greatest reduction (2%) in the cooling load of the topmost classrooms. Furthermore, the results demonstrated that the cooling energy consumption declined with the U value of the roof structure (all other parameters being held constant). While the thermal impact of roof construction was evident, it was restricted to the cooling load of only the topmost classrooms; its impact on the cooling energy consumption of the entire building was relatively insignificant. In case 6, the total cooling energy consumption of the building diminished by about 0.4%.

3.2.3. External Wall Construction. External walls are known to crucially affect building energy consumption in hot-humid areas through their impact on the cooling load [63, 64], as dictated by the materials of their envelopes and thermal insulation. In the original case, the external wall comprised ordinary bricks without thermal insulation. To improve its thermal performance, investigative modifications thus involved replacing ordinary bricks with aerated bricks and altering the thickness of the insulation layers. The results showed that improved thermal performances of the external wall contributed to cooling energy saving (Table 4). The cooling load declined with its decreasing U values: Among all the cases, the U value in case 15 was the smallest, with a resultant lowering of the cooling energy to the greatest extent (1.8%).

3.2.4. External Windows. Heat exchange through windows, determined by the thermal performance of glazing, critically influences the indoor heat balance and thus cooling load of buildings in hot-humid areas [10, 65]. Low-

Table 5: Window materials of cases 26 to 37.

Case	Window type	Total solar transmission	Light transmission	U value
Original case	Single-glaze (clear)	0.86	0.9	5.9
Case 16	Single-glaze (low-E)	0.63	0.8	3.40
Case 17	Single-glaze (low-E)	0.42	0.68	3.16
Case 18	Single-glaze (low-E)	0.37	0.75	3.05
Case 19	Double-glaze (low-E)	0.65	0.72	2.00
Case 20	Double-glaze (low-E)	0.38	0.62	1.90
Case 21	Double-glaze (low-E)	0.33	0.68	1.84
Case 22	Triple-glaze (low-E)	0.45	0.59	1.49
Case 23	Triple-glaze (low-E)	0.35	0.56	1.44
Case 24	Triple-glaze (low-E)	0.31	0.62	1.40
Case 25	Triple-glaze (low-E)	0.42	0.48	0.97
Case 26	Triple-glaze (low-E)	0.32	0.42	0.89
Case 27	Triple-glaze (low-E)	0.3	0.61	0.88

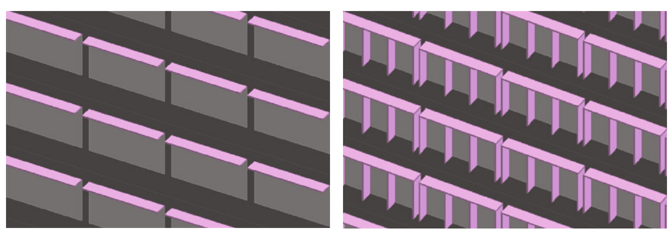

Figure 18: Horizontal and egg-crate shading devices.

emissivity and multiple-glazed windows are often used for conserving energy, given their optimal thermal and optical properties. For a given window, a smaller total solar transmittance and U value translate into less heat transfer and thus better thermal performance. In this study, modifications of the windows were undertaken for simulations (Table 5). The results showed that all the changes in the window materials reduced the cooling load. The U value exerted a nonlinear coupling impact on the cooling load: As the U value decreased, the load would not invariably exhibit the same trend. The total solar transmission of the glass exerted a more consistent impact on the cooling energy: As the transmission increased, greater consumption of energy would be incurred. Accordingly, in case 28, the low total solar transmission value and moderate U value of the window translated into its lowest cooling load (8.7% less than the original). Case 26 represented the worst among the cases, in which only 3.9% cooling energy was saved.

3.2.5. External Shading Devices. External shading devices are also deployed to limit space heat gain, with demonstrable effectiveness in lowering the cooling load in hot-humid areas [10, 46, 66]. In this study, the impacts of horizontal shading devices and egg-crate shading devices were tested on the north- and south-facing classroom windows (Figure 18). Three sizes were used (0.3 m, 0.6 m, and 0.9 m). In cases 38, 39, and 40, horizontal shading devices were installed; in cases 41, 42, and 43, egg-crate ones were installed, ranging in size from small to large. To ensure similar sizes and orientations of the windows, case 3 was used as the benchmark. The results showed that, across all six cases, an evident positive effect was noted on cooling energy consumption. In terms of the type of shading devices, egg-crate ones outperformed their horizontal counterparts in lowering the cooling load. In terms of their size, the larger ones yielded greater savings in cooling energy. case 43 was found to reduce the cooling load to the greatest extent (9.7%), followed by case 42 (8.2%), and then by case 40 (6.1%).

3.3. Comprehensive Retrofit Solution. To optimize the saving potential of the cooling load for the target building, the best-performing cases in each group (cases 3, 7, 25, 28, and 42) were integrated into a single comprehensive retrofit solution. As anticipated, the joint application of the strategies to the building yielded a favorable reduction in the cooling load by 16.6%. With such an encouraging observation, it was envisioned that the practical implementation of such an integrated retrofit solution would afford substantial savings for the annual cooling load. The cooling load and saving ratio is shown in Figure 19.

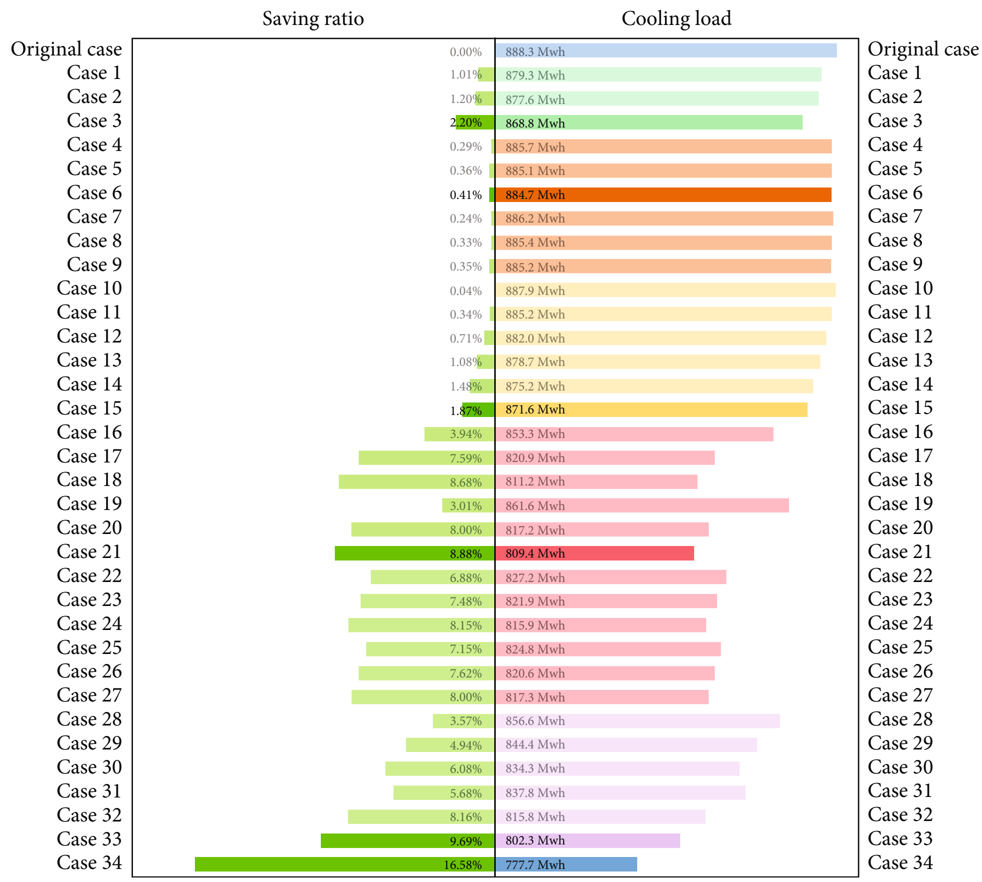

FIGURE 19: Cooling load and saving ratio.

4. Conclusions

Thermal investigations in this study were undertaken for an actual classroom building during summers in hot-humid areas of southern China, with air temperature and PMV values as evaluative indicators for thermal comfort. As shown by the simulations, overheating persisted in the naturally ventilated classrooms throughout most of the summer, potentially impairing the students' health and learning efficiency. The resultant widespread use of air conditioning for indoor cooling, alongside the substantial number of campuses and students in China, highlighted the need for reducing the cooling load.

The architectural designs of the classrooms were intertwined with their cooling load. Our findings have demonstrated that jointly applying effective retrofit strategies to the building yielded a favorable reduction in the annual cooling energy consumption by 16.6%. It follows that, when designing classroom buildings, the impacts of different strategies on energy consumption should be compared, from among which the optimal one is then to be selected. Furthermore, our findings have demonstrated that the use of external windows with glazing materials of good thermal performance and additional external shading devices were the two most effective strategies in mitigating the cooling load. Accordingly, to reduce the cooling load of classrooms in hot-humid areas, limiting heat gain from external windows should be prioritized.

Our research represents the beginning of a series of thermal investigations aiming to provide evidence-based referential guidance for building designs for classrooms in a hot-humid climate. Based on analysis of the actual classroom building, this work has updated the typical meteorological year of Guangzhou, offering evidence of the practical importance of prudent architectural designs and optimization in building retrofit. Building upon the insights herein, future works may examine the design strategies of the classrooms in hot-humid areas from the perspective of space units and building units. Additionally, climate change should be considered to improve both applicability and timeliness of the research.

Data Availability

The data used to support the findings of this study are available from the corresponding author upon request.

Conflicts of Interest

The authors declare that they have no conflicts of interest.

Acknowledgments

This study was funded by the State Key Laboratory of Subtropical Building Science (grant number 2022ZB06).

References

[1] IEA, *IEA Online Data Services*, 2013, December 2021, http://http://data.iea.org/ieastore/statslisting.asp.

[2] EC-European Commission, *New EU energy plan – More security, less pollution*, 2007, December 2021, http://ec.europa.eu/news/energy/070110.

[3] Y. Jiang and X. Yang, "China building energy consumption situation and the problems exist in the energy conservation works," *China Construction*, vol. 2, pp. 12–17, 2006, (in Chinese).

[4] B. Grassi, E. A. Piana, A. M. Lezzi, and M. Pilotelli, "A review of recent literature on systems and methods for the control of thermal comfort in buildings," *Applied Sciences*, vol. 12, no. 11, article app12115473, p. 5473, 2022.

[5] N. Fumo, "A review on the basics of building energy estimation," *Renewable and Sustainable Energy Reviews*, vol. 31, article S1364032113007892, pp. 53–60, 2014.

[6] P. Nejat, F. Jomehzadeh, M. M. Taheri, M. Gohari, and M. Z. Abd Majid, "A global review of energy consumption, CO 2 emissions and policy in the residential sector (with an overview of the top ten CO 2 emitting countries)," *Renewable and Sustainable Energy Reviews*, vol. 43, article S1364032114010053, pp. 843–862, 2015.

[7] M. Ma, W. Cai, and Y. Wu, "China Act on the Energy Efficiency of Civil Buildings (2008): A decade review," *Science of the Total Environment*, vol. 651, pp. 42–60, 2019.

[8] T. Huo, W. Cai, H. Ren et al., "China's building stock estimation and energy intensity analysis," *Journal of Cleaner Production*, vol. 207, article S0959652618330749, pp. 801–813, 2019.

[9] IEA, *Tracking Buildings 2020, IEA*, Paris, 2020December 2021, https://www.iea.org/reports/tracking-buildings-2020.

[10] M. K. Singh, R. Ooka, H. B. Rijal, S. Kumar, A. Kumar, and S. Mahapatra, "Progress in thermal comfort studies in classrooms over last 50 years and way forward," *Energy and Buildings*, vol. 188-189, pp. 149–174, 2019.

[11] A. K. Mishra and M. Ramgopal, "Thermal comfort field study in undergraduate laboratories – an analysis of occupant perceptions," *Building and Environment*, vol. 76, article S0360132314000572, pp. 62–72, 2014.

[12] N. K. Khambadkone, P. Madhumati, and M. N. Ranganath, "Thermal Comfort Evaluation in Architectural Studio Classrooms – A Summer Study in a Warm to Moderate Indian Climate," *Indoor and Built Environment*, vol. 0, p. 1420326X2210985, 2022.

[13] M. K. Singh, S. Kumar, R. Ooka, H. B. Rijal, G. Gupta, and A. Kumar, "Status of thermal comfort in naturally ventilated classrooms during the summer season in the composite climate of India," *Building and Environment*, vol. 128, article S0360132317305395, pp. 287–304, 2018.

[14] H. Koch-Nielsen, *Stay Cool: A Design Guide for the Built Environment in Hot Climates*, Routledge, London, UK, 1st edition, 2013.

[15] J. C. Lam, K. K. W. Wan, C. L. Tsang, and L. Yang, "Building energy efficiency in different climates," *Energy Conversion and Management*, vol. 49, no. 8, article S0196890408000393, pp. 2354–2366, 2008.

[16] W. I. Wan Mohd Nazi, M. Royapoor, Y. Wang, and A. P. Roskilly, "Office building cooling load reduction using thermal analysis method – A case study," *Applied Energy*, vol. 185, article S0306261915016268, pp. 1574–1584, 2017.

[17] L. Hou, Y. Liu, L. Yang, J. Liu, and Y. Qiao, "The impacts of energy efficiency design parameters on office buildings energy consumption in different climate zones in China," *Procedia Engineering*, vol. 205, article S1877705817345356, pp. 2478–2484, 2017.

[18] A. K. K. Lau, E. Salleh, C. H. Lim, and M. Y. Sulaiman, "Potential of shading devices and glazing configurations on cooling energy savings for high-rise office buildings in hot-humid climates: the case of Malaysia," *International Journal of Sustainable Built Environment*, vol. 5, no. 2, article S2212609016300176, pp. 387–399, 2016.

[19] China Statistical YearbookMay 2021, http://www.stats.gov.cn/tjsj/ndsj/2019/indexeh.htm.

[20] S. Papadopoulos, C. E. Kontokosta, A. Vlachokostas, and E. Azar, "Rethinking HVAC temperature setpoints in commercial buildings: the potential for zero-cost energy savings and comfort improvement in different climates," *Building and Environment*, vol. 155, article S036013231930232X, pp. 350–359, 2019.

[21] M. A. Aktacir, O. Büyükalaca, and T. Yılmaz, "A case study for influence of building thermal insulation on cooling load and air-conditioning system in the hot and humid regions," *Applied Energy*, vol. 87, no. 2, article S0306261909002062, pp. 599–607, 2010.

[22] L. Shi and M. Y. L. Chew, "A review on sustainable design of renewable energy systems," *Renewable and Sustainable Energy Reviews*, vol. 16, no. 1, article S1364032111003947, pp. 192–207, 2012.

[23] S. B. Sadineni, S. Madala, and R. F. Boehm, "Passive building energy savings: a review of building envelope components," *Renewable & Sustainable Energy Reviews*, vol. 15, no. 8, article S1364032111002504, pp. 3617–3631, 2011.

[24] C. E. Ochoa and I. G. Capeluto, "Strategic decision-making for intelligent buildings: comparative impact of passive design strategies and active features in a hot climate," *Building & Environment*, vol. 43, no. 11, article S0360132307002090, pp. 1829–1839, 2008.

[25] Y. Zou, K. Xiang, Q. Zhan, and Z. Li, "A simulation-based method to predict the life cycle energy performance of residential buildings in different climate zones of China," *Building and Environment*, vol. 193, article S0360132321000743, p. 107663, 2021.

[26] L. Belussi, B. Barozzi, A. Bellazzi et al., "A review of performance of zero energy buildings and energy efficiency solutions," *Journal of building engineering*, vol. 25, p. 100772, 2019.

[27] Y. Zou, Q. Zhan, and K. Xiang, "A comprehensive method for optimizing the design of a regular architectural space to improve building performance," *Energy Reports*, vol. 7, article S2352484721001013, pp. 981–996, 2021.

[28] T. Lim, W. S. Yim, and D. D. Kim, "Evaluation of daylight and cooling performance of shading devices in residential buildings in South Korea," *Energies*, vol. 13, no. 18, article en13184749, p. 4749, 2020.

[29] A. M. Omer, "Renewable building energy systems and passive human comfort solutions," *Renewable and Sustainable Energy*

Reviews, vol. 12, no. 6, article S1364032106001055, pp. 1562–1587, 2008.

[30] Y. Zhang, "Design criteria of built thermal environment for hot summer & warm winter zone of China," *Building and Environment*, vol. 88, article S0360132314003680, pp. 97–105, 2015.

[31] V. Cheng and E. Ng, "Comfort temperatures for naturally ventilated buildings in Hong Kong," *Architectural Science Review*, vol. 49, no. 2, pp. 179–182, 2006.

[32] P. Fanger, *Thermal Comfort*, Danish Technical Press, Copenhagen, Denmark, 1970.

[33] R. De Dear and G. S. Brager, "Developing an adaptive model of thermal comfort and preference," in *Proceedings of the ASHRAE annual winter meeting 1998*, San Francisco, USA, January 1998.

[34] ASHRAE, *Standard 55-2017, Thermal Environment Conditions for Human Occupancy*, ASHRAE, Atlanta, 2017.

[35] J. van Hoof, "Forty years of Fanger's model of thermal comfort: comfort for all?," *Indoor Air*, vol. 18, no. 3, pp. 182–201, 2008.

[36] R. J. de Dear and G. S. Brager, "Thermal comfort in naturally ventilated buildings: revisions to ASHRAE standard 55," *Energy and Buildings*, vol. 34, no. 6, article S0378778802000051, pp. 549–561, 2002.

[37] P. Ole Fanger and J. Toftum, "Extension of the PMV model to non-air-conditioned buildings in warm climates," *Energy and Buildings*, vol. 34, no. 6, article S0378778802000038, pp. 533–536, 2002.

[38] Y. Zhang, J. Wang, H. Chen, J. Zhang, and Q. Meng, "Thermal comfort in naturally ventilated buildings in hot-humid area of China," *Building and Environment*, vol. 45, no. 11, article S0360132310001733, pp. 2562–2570, 2010.

[39] EnergyPlusMarch 2021, https://energyplus.net/.

[40] Y. P. Zhou, J. Y. Wu, R. Z. Wang, S. Shiochi, and Y. M. Li, "Simulation and experimental validation of the variable-refrigerant-volume (VRV) air-conditioning system in EnergyPlus," *Energy and Buildings*, vol. 40, no. 6, article S0378778807002216, pp. 1041–1047, 2008.

[41] Y. Xu, C. Yan, H. Qian, L. Sun, G. Wang, and Y. Jiang, "A novel optimization method for conventional primary and secondary school classrooms in southern China considering energy Demand, Thermal Comfort and Daylighting," *Thermal Comfort and Daylighting. Sustainability*, vol. 13, no. 23, article su132313119, p. 13119, 2021.

[42] N. M. Mateus, A. Pinto, and G. C. D. Graça, "Validation of EnergyPlus thermal simulation of a double skin naturally and mechanically ventilated test cell," *Energy and Buildings*, vol. 75, article S0378778814001571, pp. 511–522, 2014.

[43] R. H. Henninger, M. J. Witte, and D. B. Crawley, "Analytical and comparative testing of EnergyPlus using IEA HVAC BESTEST E100–E200 test suite," *Energy and Buildings*, vol. 36, no. 8, article S0378778804000362, pp. 855–863, 2004.

[44] S. S. M. D. Shrestha, *Empirical validation of building energy simulation software: EnergyPlus*, O. R. T. U. O. R. N. Lab ORNL and B. T. R. A. Center, Eds., Iowa State University, 2011.

[45] E. Vuong, R. S. Kamel, and A. S. Fung, "Modelling and simulation of BIPV/T in EnergyPlus and TRNSYS," *Energy Procedia*, vol. 78, article S187661021502086X, pp. 1883–1888, 2015.

[46] A. D. Fontanini, J. L. Castro Aguilar, M. S. Mitchell et al., "predicting the performance of radiant technologies in attics: reducing the discrepancies between attic specific and whole-building energy models," *Energy and Buildings*, vol. 169, article S0378778817337544, pp. 69–83, 2018.

[47] Y. T. Kwok, A. K. L. Lai, K. K. L. Lau et al., "Thermal comfort and energy performance of public rental housing under typical and near-extreme weather conditions in Hong Kong," *Energy and Buildings*, vol. 156, article S0378778817314822, pp. 390–403, 2017.

[48] A. L. S. Chan and T. T. Chow, "Investigation on energy performance and energy payback period of application of balcony for residential apartment in Hong Kong," *Energy and Buildings*, vol. 42, no. 12, article S0378778810002719, pp. 2400–2405, 2010.

[49] A. L. S. Chan, "Effect of adjacent shading on the thermal performance of residential buildings in a subtropical region," *Applied Energy*, vol. 92, article S0306261911007690, pp. 516–522, 2012.

[50] W. K. Alhuwayil, M. Abdul Mujeebu, and A. M. M. Algarny, "Impact of external shading strategy on energy performance of multi-story hotel building in hot-humid climate," *Energy*, vol. 169, article S0360544218324356, pp. 1166–1174, 2019.

[51] DesignBuilder Software Ltd-HomeJanuary 2021, https://designbuilder.co.uk/.

[52] A. Ebrahimpour and M. Maerefat, "A method for generation of typical meteorological year," *Energy Conversion and Management*, vol. 51, no. 3, article S0196890409003902, pp. 410–417, 2010.

[53] A. Amillo, T. Huld, and R. Müller, "A new database of global and direct solar radiation using the eastern Meteosat satellite, models and validation," *Models and Validation. Remote Sensing*, vol. 6, no. 9, article rs6098165, pp. 8165–8189, 2014.

[54] I. J. Hall, R. R. Prairie, H. E. Anderson, and E. C. Boes, "Generation of a Typical Meteorological Year," in *Proceedings of the 1978 annual meeting of the American Section of the International, Solar Energy Society*, pp. 669–671, San Diego, CA, USA, 1978.

[55] S. Wilcox and W. Marion, *Users Manual for tmy3 Data Sets*, National Renewable Energy Lab. (NREL),, Golden, CO (United States), 2008.

[56] D. Pissimanis, G. Karras, V. Notaridou, and K. Gavra, "The generation of a "Typical meteorological year" for the city of Athens," *Solar Energy*, vol. 40, no. 5, article 0038092X88900953, pp. 405–411, 1988.

[57] N. M. Nahar, P. Sharma, and M. M. Purohit, "Performance of different passive techniques for cooling of buildings in arid regions," *Building and Environment*, vol. 38, no. 1, article S036013230200029X, pp. 109–116, 2003.

[58] A. Synnefa, M. Santamouris, and H. Akbari, "Estimating the effect of using cool coatings on energy loads and thermal comfort in residential buildings in various climatic conditions," *Energy and Buildings*, vol. 39, no. 11, article S0378778807000126, pp. 1167–1174, 2007.

[59] M. D'Orazio, C. Di Perna, and E. Di Giuseppe, "The effects of roof covering on the thermal performance of highly insulated roofs in Mediterranean climates," *Energy and Buildings*, vol. 42, no. 10, article S0378778810001234, pp. 1619–1627, 2010.

[60] N. H. Wong, D. K. W. Cheong, H. Yan, J. Soh, C. L. Ong, and A. Sia, "The effects of rooftop garden on energy consumption of a commercial building in Singapore," *Energy and Buildings*, vol. 35, no. 4, article S0378778802001081, pp. 353–364, 2003.

[61] A. Mahmoud, M. Asif, M. Hassanain, M. Babsail, and M. Sanni-Anibire, "Energy and economic evaluation of green roofs for residential buildings in hot-humid climates," *Buildings*, vol. 7, no. 4, article buildings7020030, p. 30, 2017.

[62] C. Y. Jim and L. L. H. Peng, "Weather effect on thermal and energy performance of an extensive tropical green roof," *Urban Forestry & Urban Greening*, vol. 11, no. 1, article S1618866711000914, pp. 73–85, 2012.

[63] D. Pan, M. Chan, S. Deng, and Z. Lin, "The effects of external wall insulation thickness on annual cooling and heating energy uses under different climates," *Applied Energy*, vol. 97, article S0306261911008038, pp. 313–318, 2012.

[64] Z. Fang, N. Li, B. Li, G. Luo, and Y. Huang, "The effect of building envelope insulation on cooling energy consumption in summer," *Energy and Buildings*, vol. 77, article S0378778814002503, pp. 197–205, 2014.

[65] I. Iqbal and M. S. Al-Homoud, "Parametric analysis of alternative energy conservation measures in an office building in hot and humid climate," *Building and Environment*, vol. 42, no. 5, article S0360132306001119, pp. 2166–2177, 2007.

[66] A. A. Touma and D. Ouahrani, "Shading and day-lighting controls energy savings in offices with fully-glazed façades in hot climates," *Energy and Buildings*, vol. 151, article S0378778817302487, pp. 263–274, 2017.